OXFORD

Cerebral Cortex, 2019;00: 1–18

doi: 10.1093/cercor/bhz202
Advance Access Publication Date:
Original Article

ORIGINAL ARTICLE

Focused Representation of Successive Task Episodes in Frontal and Parietal Cortex

Mikiko Kadohisa[1], Kei Watanabe[2,3], Makoto Kusunoki[1], and Mark J Buckley[2] and John Duncan[1,2]

[1]MRC Cognition and Brain Sciences Unit, University of Cambridge, Cambridge CB2 7EF, UK, [2]Department of Experimental Psychology, University of Oxford, Oxford OX1 3UD, UK, [3]Graduate School of Frontier Biosciences, Osaka University, Osaka 565-0871, Japan

Address correspondence to email: miki.kadohisa@psy.ox.ac.uk.

Abstract

Complex cognition is dynamic, with each stage of a task requiring new cognitive processes appropriately linked to stimulus or other content. To investigate control over successive task stages, we recorded neural activity in lateral frontal and parietal cortex as monkeys carried out a complex object selection task, with each trial separated into phases of visual selection and learning from feedback. To study capacity limitation, complexity was manipulated by varying the number of object targets to be learned in each problem. Different task phases were associated with quasi-independent patterns of activity and information coding, with no suggestion of sustained activity linked to a current target. Object and location coding were largely parallel in frontal and inferior parietal cortex, though frontal cortex showed somewhat stronger object representation at feedback, and more sustained location coding at choice. At both feedback and choice, coding precision diminished as task complexity increased, matching a decline in performance. We suggest that, across successive task steps, there is radical but capacity-limited reorganization of frontoparietal activity, selecting different cognitive operations linked to their current targets.

Key words: attention, cognitive control, frontal, parietal, working memory

Introduction

Much evidence shows joint activity of frontal and parietal cortex in complex cognitive activities. Human imaging studies show co-recruitment of lateral frontal and parietal cortex during tasks of many kinds, generally as part of a wider "multiple-demand" or cognitive control network including also regions of dorsomedial frontal and insular cortex (e.g., Cabeza and Nyberg 2000; Duncan 2010). Lateral frontal and inferior parietal cortex have direct anatomical connections (Petrides and Pandya 1984; Cavada and Goldman-Rakic 1989), and neurophysiological studies suggest bidirectional flow of information between them (e.g., Buschman and Miller 2007; Salazar et al. 2012; Crowe et al. 2013). In the behaving monkey, similar response patterns have often been described in neurons of lateral frontal cortex and parietal regions including Lateral intraparietal and the adjacent convexity (Chafee and Goldman-Rakic 1998; Freedman et al. 2001; Goodwin et al. 2012; Salazar et al. 2012; Rishel et al. 2013; Brincat et al. 2018), and when differences are found, they are usually quantitative, against a background of broadly similar behavior (e.g., Buschman and Miller 2007; Suzuki and Gottlieb 2013; Meyers et al. 2018).

It is widely accepted that frontoparietal activity reflects "cognitive control," but much remains open in how control should be conceived. Following the early thinking of Fuster (1989) and Goldman-Rakic (1988)), one well-established aspect is information maintenance in working memory. In the classical delayed

response task, for example, a cue indicates the target location for future behavior, and after a brief delay, the animal makes a reach or saccade to that location. In this task, neurons of both lateral frontal and parietal cortex can show a prominent pattern of sustained activity, maintaining information concerning the target location between initial presentation and response (Fuster and Alexander 1971; Gnadt and Andersen 1988; Funahashi et al. 1989; for recent review and discussion, see Constantinidis et al. 2018; Lundqvist et al. 2018). Similar findings concern working memory for object features or categories in the delay period of delayed match-to-sample tasks (e.g., Fuster et al. 1982; Freedman et al. 2001; Freedman and Assad 2006). As one key aspect of cognitive control, sustained information maintenance in working memory allows the animal to escape from the context of the immediate sensory environment (e.g., Goldman-Rakic 1988).

Complex cognitive control, however, requires much more than maintained information in working memory (Miller 2000; Rigotti et al. 2010; Duncan 2013; Mante et al. 2013). In complex behavior, goals are generally achieved in a series of component steps. Some evidence suggests that, across the successive steps of a task, neural activity in prefrontal cortex radically reorganizes, such that firing patterns in successive task steps can be approximately independent or orthogonal (Sigala et al. 2008). Contrary to a simple pattern of sustained firing, even single neurons can show different stimulus selectivity at different task steps (e.g., Genovesio et al. 2006; Sigala et al. 2008; Warden and Miller 2010; Hussar and Pasternak 2012; Rigotti et al. 2013; Stokes et al. 2013; Naya et al. 2017; Parthasarathy et al. 2017; Cavanagh et al. 2018; Wasmuht et al. 2018; for similar data from rodent parietal cortex, see Raposo et al. 2014). Such results exemplify nonlinear mixed selectivity, that is, selective response to particular information occurring in a specific role or context (e.g., Mushiake et al. 2006; Rigotti et al. 2013; Chiang and Wallis, 2018). With changes in context, there can be changed patterns of functional connectivity in prefrontal cortex, suggesting construction of different functional coalitions (Lapish et al. 2008; Buschman et al. 2012; Oemisch et al. 2015). Such results make sense if patterns of activity in frontoparietal cortex serve to assemble the different cognitive processes of successive task steps, in part by directing activity in other relevant brain systems. Different processes, implemented in different brain structures, will likely require different control inputs, and very plausibly, unrelated patterns of activity will be needed to bind the same stimulus information to different cognitive operations. Activity selective for conjunctions of stimulus input and cognitive context may implement the classic computational requirement of variable binding, or linking the contents of a cognitive structure to their correct roles (e.g., Smolensky 1990).

Complementary to focus on a single task step is the effect of overall task complexity. Many behavioral studies show the impact of task complexity, from declining performance with more objects in visual working memory (Bundesen 1990; Luck and Vogel 1997), to neglect of some task rules with increasing complexity of the remainder (Duncan et al. 2008). As neural representations are created for each step of a complex task, their accuracy may be limited by the complexity of the whole. In frontal cortex, indeed, the precision of encoding for any one task element can decline with increase in total amount of information to be stored and used (Buschman et al. 2011; Watanabe and Funahashi 2014), matching many suggestions that, to some degree, frontoparietal cortex may act as a limited-capacity processor (Dehaene et al. 2003; Marois and Ivanoff 2005; Buschman et al. 2011).

In the present study, we embedded a classic delay task within a more complex task structure (cf. Watanabe and Funahashi 2014). Neural activity was recorded simultaneously across several regions of lateral frontal and parietal cortex. Our aim was to compare patterns of activity and information coding in separate task steps, and at the same time, to assess effects of task complexity. On each trial, the monkey reached to and touched one of four objects presented on a touchscreen. Of the four objects used for any given problem, one or two were targets, bringing reward when selected, while the remainder were nontargets. For each problem, accordingly, the monkey's task was to learn by initial sampling which objects were targets, and then repeatedly to reselect these until a new problem began. We examined activity in two phases of the trial. Following each touch, a feedback signal indicated whether the selected object was a target or not. Analogous to the sample stimulus in a delayed match-to-sample task, we regarded this as an instruction, indicating what behavior would be rewarded on future trials. At this phase, the requirement was to store the information received as guidance for future choices. The second phase of interest was the choice itself, when, following initial learning, the animal selected one of four objects in a current display to be touched. Here, analogous to the test phase of delayed match-to-sample, the requirement was to retrieve target information from memory and use it to guide selection among the available alternatives. To address the dynamics of successive cognitive operations, we examined profiles and timing of neural activity and information coding at feedback and choice. To address limitations on representational capacity, we compared behavior and neural coding in one- and two-target tasks.

Materials and Methods

Subjects

Subjects were two male rhesus monkeys (*Macaca mulatta*), each weighing 13 kg. The experiments were performed in accordance with the Animals (Scientific Procedures) Act 1986 of the UK; all procedures were licensed by a Home Office Project License obtained after review by Oxford University's Animal Care and Ethical Review committee, and were in compliance with the guidelines of the European Community for the care and use of laboratory animals (EUVD, European Union directive 86/609/EEC).

Task

Task events were controlled by REX real-time data acquisition and laboratory control software (developed by the National Institutes of Health), with displays presented on a 17.5 inch LED touch screen placed in front of the monkey's chair. A start key was attached to the front of the chair.

In each session, the animal worked through a series of problems, each consisting of four cycles of trials (Fig. 1A, top). In each trial (Fig. 1A, bottom), the animal was shown a visual display of four objects. For each animal, there were two four-object sets (Fig. 1A, inset), fixed across the experiment, and used in alternate problems throughout the session. Each display contained all four objects from the current set, randomly placed. On receipt of a go signal, the animal released a start key and selected one object by touching it. In each problem, one (1T problems) or two (2T problems) objects from the current set were defined as targets. If the object touched on the current trial was a target,

this was followed by reward; if it was a nontarget, the touch led to a negative feedback signal and no reward. Thus, in cycle 1 of each problem, the animal had to work through a series of trials, sampling objects at random until the target or targets were discovered. In subsequent cycles, the optimal performance was to re-select targets and avoid nontargets. Trials continued in each cycle until all targets (one or two) had been touched once, after which the next cycle began. For each target, reward was only available the first time it was touched within each cycle; revisits brought negative feedback and no reward. Thus, following target discovery in cycle 1, each subsequent cycle consisted optimally of just a single trial for a 1T problem, and of two trials, one for selection of each target, for a 2T problem. In the 2T case, the animal was free to select the two targets in each cycle in either order. 1T and 2T problems were blocked in each session (mean of 69 1T and 67 2T problems per session), so that animals knew the current number of targets to be discovered. Additional cues reinforced the animal's knowledge of when each cycle and each problem were completed (see below).

Details of events on each trial are illustrated in Figure 1A (bottom). Before the trial began, the screen showed a central white fixation point (FP) and a surrounding display of four black squares (each square 5.7° × 5.7° visual angle, centered 11.4° from fixation). To initiate trial events, the monkey was required to press and hold down the start key, and to acquire and hold central fixation (window 7.6° × 7.6°). At this point, the FP turned red, and there was a wait period of 0.8–1.2 s, after which the black squares were replaced by a display (CH) of four choice objects. Following a further delay of 1.2–2.0 s, the FP changed to cyan (GO) to indicate that a response could be made. To indicate his choice, the animal released the home key (key release, KR) and touched one of the objects (touch required within 1.8 s of GO). After the touch had been held for 0.35–0.45 s, the selected object was replaced by either a green (target; see below) or red (nontarget) square (feedback, FB), which remained for 0.3 s followed by an intertrial display (see below). If the touched object was a target, a drop of soft food (reward, RW) was delivered 0.05–0.15 s after FB offset. Once a trial had been initiated, it was aborted without RW if the monkey released the start key or broke fixation prior to GO. The trial was also aborted if, after an object had been touched, the touch was not maintained until FB.

Different intertrial displays indicated transitions within a cycle, between cycles, and between problems. For trials within a cycle, the intertrial display was simply the white FP and surrounding black squares (see Fig. 1A), with a minimum period of 0.7–0.9 s required before the next trial would begin. To indicate the end of a cycle, this display was preceded by a period of only the white FP, lasting 3.2–3.5 s. To indicate the end of a problem, the screen blanked for 3.3–3.6 s.

Recordings

Each monkey was implanted with a titanium head holder and recording chambers (Gray Matter Research), fixed on the skull with stainless steel screws. Frontal chambers were placed over the lateral prefrontal cortex of the right hemisphere for both monkey A (AP = 33.9, ML = 20.3; AP, anterior–posterior; ML, medio-lateral) and monkey B (AP = 36.2, ML = 58.1). Posterior chambers were placed over the parietal cortex of the right hemisphere for both monkey A (AP = −4.6, ML = 50.6) and monkey B (AP = −3.2, ML = 47.4). Recording locations for each animal are shown in Figure 1B. A craniotomy was made under each chamber for physiological recording. All surgical procedures were aseptic and carried out under general anesthesia.

Data were recorded over a total of 59 daily sessions. For each chamber, we used a 32 channel semichronic microdrive system (SC-32, Gray Matter Research) with 1.5 mm interelectrode spacing, interfaced to a multichannel data acquisition system (Cerebus System, Blackrock Microsystems). Between sessions, to ensure recording of new cells, electrodes were advanced by a minimum of 62.5 µm. Neural activity was amplified, filtered (300 Hz to 10 kHz), and stored for offline cluster separation and analysis (Offline Sorter, Plexon). Eye position was sampled at the rate of 120 Hz using an infrared eye tracking system (Applied Science Laboratories) and stored for offline analysis. We did not preselect neurons for task-related responses; instead, we advanced microelectrodes until we could isolate neuronal activity before starting the task.

At the end of the experiments, animals were deeply anesthetized with barbiturate and then perfused through the heart with heparinized saline followed by 10% formaldehyde in saline. The brains were removed for histology and recording locations confirmed (Fig. 1B).

Data and Analysis

All statistical analyses were carried out using MATLAB (MathWorks). For each recording region, we used ANOVAs on multiple time windows (see Results) to assess coding of object and location information. One measure was the proportion of all recorded cells with a significant main effect ($P < 0.05$). The other was the mean proportion of explained variance (PEV), averaged across recorded cells. PEV was measured by the partial ω^2 index of effect size, calculated by the formula

$$\omega^2 = df_{\text{effect}} \times (\text{MS}_{\text{effect}} - \text{MSE}) \,/\, (\text{SS}_{\text{effect}} + (\text{N}_{\text{total}} - df_{\text{effect}}) \times \text{MSE}), \quad (1)$$

where df_{effect} is degrees of freedom for the factor of interest (object, location), $\text{MS}_{\text{effect}}$ is the mean square for the factor, $\text{SS}_{\text{effect}}$ is the sum of squares for the factor, MSE is the mean square error, and N_{total} is the total number of observations (trials).

Randomization tests were used to assess the significance of mean PEV values across cells within one region (Figs 4A, 4C, 5, and 7A). For each cell, labels (objects or locations) were randomized across trials, followed by re-calculation of mean PEV across cells. The PEV value for the true data was compared with the distribution obtained from 1000 repetitions of this randomization, and the p value determined by the proportion of randomized values greater than or equal to the true value. The criterion for significance was set at $p < 0.05$ corrected for multiple comparisons (time windows) by Holm-Bonferroni.

For comparison of PEVs between regions (Figs 4A and 7A) or conditions (Figs 4B and 8A), we used Wilcoxon rank-sum tests for between regions, and Wilcoxon signed-rank test for between conditions. As expected, for both object and location coding, there were many nonselective cells (PEV close to zero), with a tail of cells carrying more information. For each statistical comparison, we focused just on the 25% of most selective cells. For comparison between regions, these were the 25% of cells from each region with highest PEV. For comparison between conditions, the top 25% were selected from an ANOVA combining data from the two conditions. For each comparison, the crite-

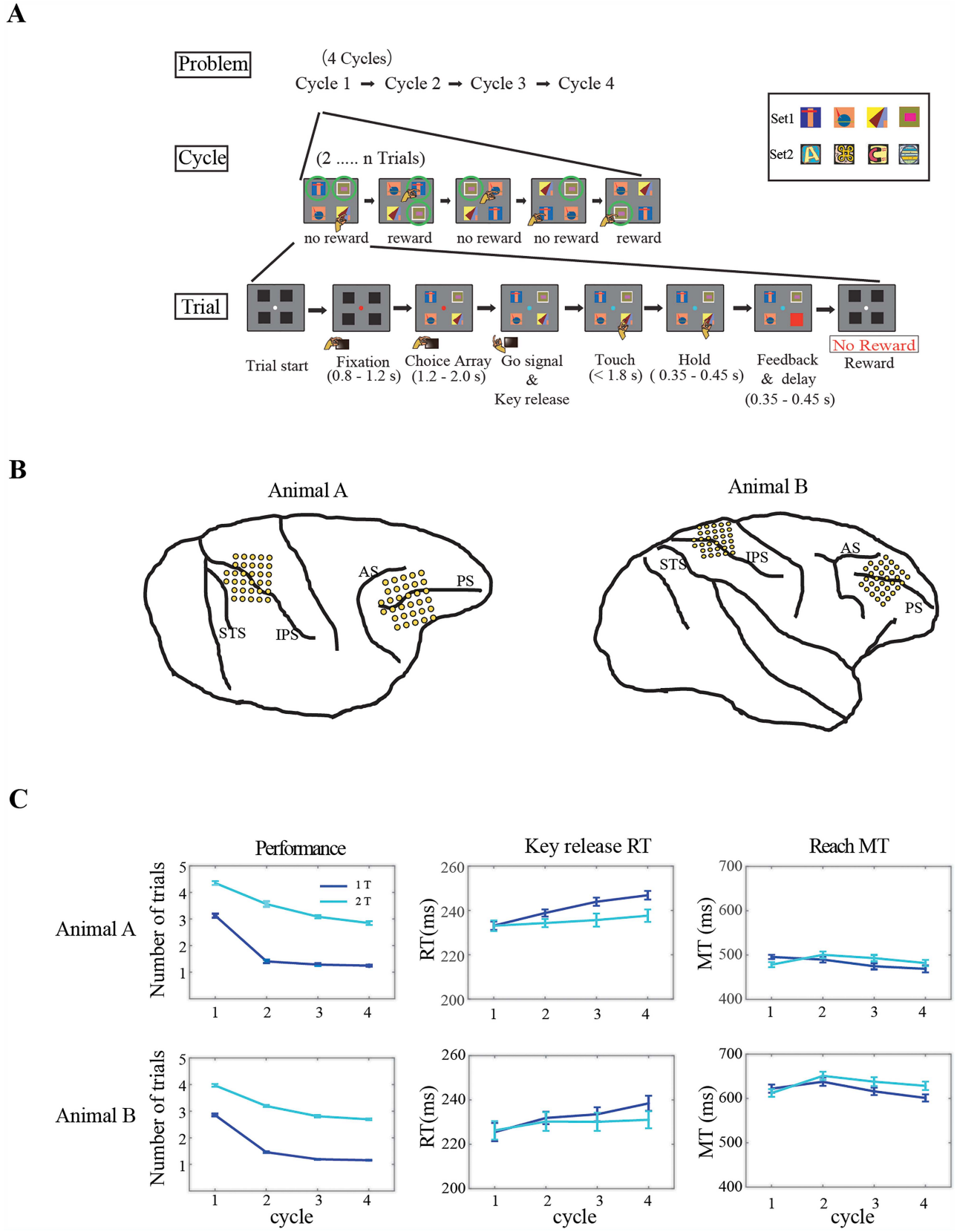

Figure 1. Task, behavior, and recordings. (*A*) Illustration of two-target (2 T) task. Each problem was based on a set of four objects, with two fixed four-object sets alternating between problems for each animal (object sets for one animal illustrated in inset). For each problem, two objects were targets (green circles, not visible on actual display). Touching a target brought reward, whereas touching a nontarget brought no reward. One target was touched per trial; on cycle 1 of each problem, the animal was required to explore until the targets were discovered, while on later cycles, the optimal behavior was to touch just the targets learned in cycle 1. Within each cycle, reward could be obtained from each target only once (see no reward for fourth trial of the illustrated cycle). In one-target (1T) problems, events were similar, but with only a single target to be discovered. (*B*) Recording locations for the two animals. Note that, to increase cell capture in animal A, the frontal array was repositioned (rotated) once within the chamber midway through the experiment; the figure shows electrode locations before this rotation. AS: arcuate sulcus; IPS: intraparietal sulcus; PS: principal sulcus; and STS: superior temporal sulcus. (*C*) Behavioral data. Left panel: mean number of trials (object touches) per cycle. Middle panel: mean reaction time (RT) to release the key following go signal. Right panel: mean MT from KR to object touch.

rion for significance was set at $P < 0.05$ corrected for multiple comparisons (time windows) by Holm-Bonferroni.

To calculate averages across selected groups of correlations from the matrices in Figure 2, we converted each correlation to a z score, averaged these zs, then transformed the average z back to r.

For single-neuron peristimulus time histograms (Fig. 3), spike data were smoothed with a Gaussian kernel of SD 15 ms, cutoffs ± 2 SD. All other analyses were carried out on unsmoothed data.

Results

Behavioral data appear in Figure 1C. In both animals, performance on 1T problems was close to optimal across cycles 2–4, whereas in 2T problems, there was only slow improvement over cycles, never approaching the optimum. Key reaction time (RT) was in the range 220–250 ms for both animals, while time from release to object touch (movement time or MT) was around 500 ms for animal A, 600 ms for animal B.

In the frontal lobe, recordings were made on dorsal and ventral frontal convexities, and within the principal sulcus (Fig. 1B). In the parietal lobe, recordings were made on the surface of the superior and inferior parietal lobules, and within the intraparietal sulcus. For analysis, frontal lobe data were divided into ventral and dorsal regions, divided at the fundus of the principal sulcus. Parietal lobe data were divided into superior (MIP/area 5) and inferior (LIP/area 7) regions, divided at the fundus of the intraparietal sulcus. In total, we recorded the activities of 236 neurons in the prefrontal cortex (86 dorsal, 47/39 respectively from animals A/B; 150 ventral, 104/46 from A/B) and of 368 neurons in the posterior parietal cortex (174 inferior, 98/76 from A/B; 194 superior, 115/79 from A/B).

Analysis focused on two trial periods (Fig. 1A, bottom). At feedback (FB), the FB signal indicated whether the selected object was a target, to be revisited in subsequent cycles, or a nontarget, to be avoided. The signal thus served as an instruction indicating the rules of the current problem. FB activity was analyzed across all cycles 1–4. At choice (CH), the animal inspected a visual display and decided which object to touch. As animals did not know which objects were targets in cycle 1, we analyzed CH activity only for cycles 2–4. Analyses of neurophysiological data used just correct trials, that is, object touches followed by positive FB and RW.

Independent Patterns of Neural Activity at FB and CH

To provide an initial view of relations between FB and CH activity, we used the correlation approach of Sigala et al. (2008). Across the whole population of recorded neurons in each region, we compared profiles of activity in FB and CH.

For this analysis, for each cell, we measured mean activity for each combination of object × cycle (all cycles for FB, cycles 2–4 only for CH) × task phase (FB, CH), combining data from 1T and 2T problems. To capture activity surrounding the FB signal, we used average spike rate in an analysis window of −200 to +400 from FB onset. To capture activity relating to discovery of the target in the CH display, we used a window of +200 to +800 ms from CH onset. To normalize for overall firing rate differences, each value was divided by the mean spike rate for that cell, across the entire duration of the trial (−1000 ms from trial initiation to +1200 ms from FB), averaged across every trial in the session. For each recording region, the result was a vector of n values per combination of object × cycle × phase, where n is the total number of recorded cells in that region. Correlations between these vectors are shown in Figure 2A. For each region, results show consistent, quasi-independent activity patterns for FB and CH phases. Within each phase, correlations for different objects and cycles were strongly positive. Across phases, correlations were close to zero (for discussion of small negative correlations induced by mean normalization, see Sigala et al. 2008).

The data also give initial indications of object selectivity at each phase. In Figure 2A, such selectivity is shown by additional stripes parallel to the main diagonal, indicating that, between cycles, correlations were stronger for trials with the same target object. Such stripes are discernible especially in the FB period; in this period, for dorsal frontal cortex, mean correlations (see Materials and Methods) were 0.60 for same object, different cycles as compared with 0.51 for different object, different cycles; corresponding values were 0.72 and 0.63 for ventral frontal cortex, 0.64 and 0.60 for inferior parietal cortex, 0.70 and 0.66 for superior parietal cortex. In the CH period, corresponding values were 0.67 (same object, different cycles) and 0.61 (different objects, different cycles) in dorsal frontal cortex, 0.67 and 0.63 in ventral frontal cortex, 0.66 and 0.60 in inferior parietal cortex, 0.69 and 0.62 in superior parietal cortex.

In Figure 2B, theanalysis has been repeated, but now categorizing CH activity by target location rather than object. Indicating stronger location than object coding, striping is now clearly visible in CH data. In dorsal frontal cortex, mean correlations were 0.69 for same location, different cycles as compared with 0.56 for different location, different cycles; corresponding values were 0.72 and 0.52 for ventral frontal cortex, 0.66 and 0.52 for inferior parietal cortex, 0.65 and 0.59 for superior parietal cortex. More detailed analysis of object and location coding follows below.

Single neuron examples in Figure 3 illustrate the variability of neural activity between task phases. Figure 3A shows illustrative object-selective cells, two from dorsal frontal cortex (left panels) and two from inferior parietal cortex (right panels). In the upper frontal cell, there is strong response and object selectivity at FB, with little activity at CH. The lower frontal cell shows the complementary pattern, with object selectivity at CH but little activity at FB. The upper parietal cell shows a brief response following both FB and CH, but object selectivity only at FB. The lower parietal cell is significantly object-selective in both trial periods, though preferred objects in the two periods are different. Figure 3B shows example cells with location selectivity at CH (left – ventral frontal, right – inferior parietal). Following onset of the CH display, location-selective activity appears at a latency around 200 ms for the frontal cell, 300–400 ms for the parietal cell, and is then sustained through the following delay period. For this frontal cell, there is little activity in the FB period, while for the parietal cell, there is also significant location selectivity at FB, but with different preferred locations at FB and CH. Resembling the results of Sigala et al. (2008), these data show quasi-independent patterns of activity for FB and CH phases. Against this background, object and location information are encoded as small modulations of basic task-phase patterns.

Instructing the Current Rules: Object-Selective Activity at Feedback

For the next step, we focused on object encoding around the time of FB. To this end, we performed ANOVAs on the data from

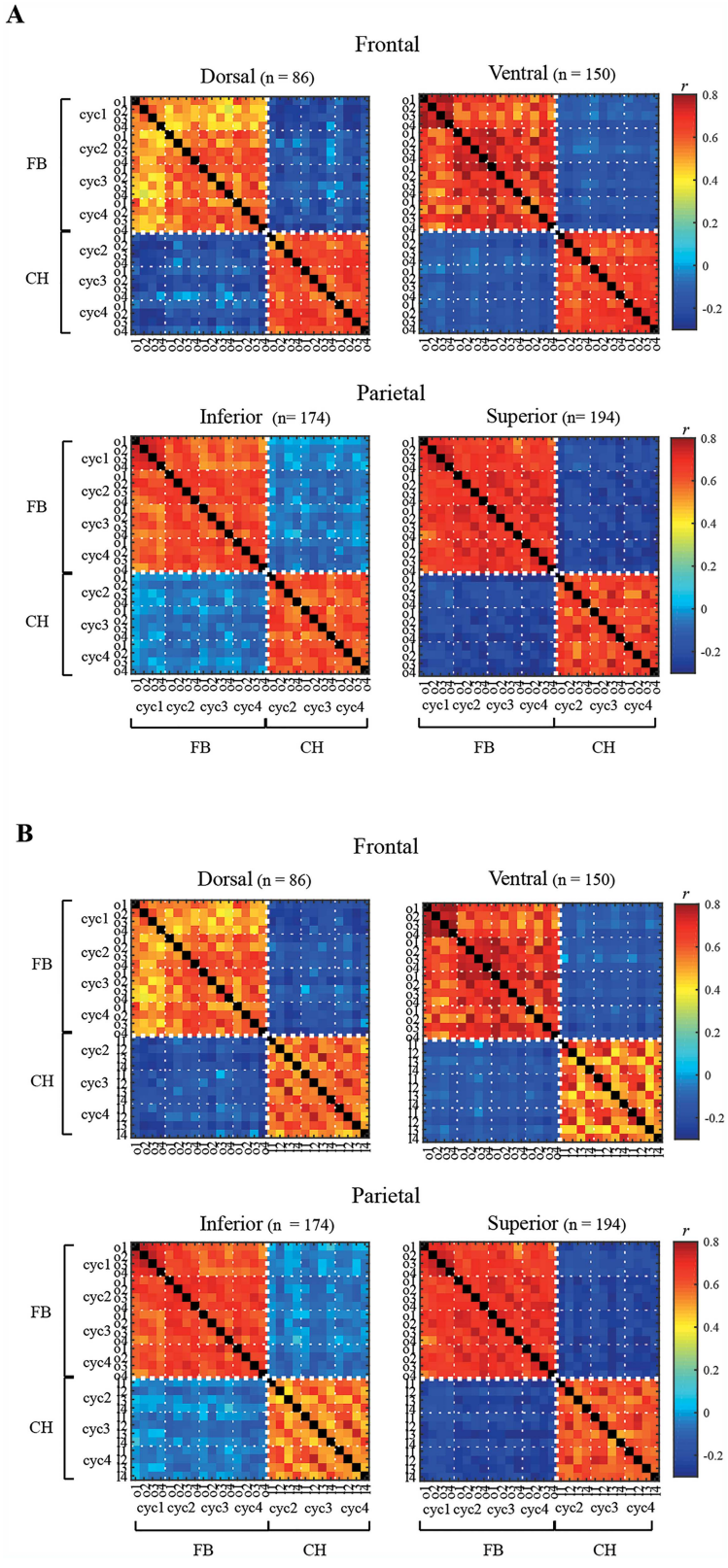

Figure 2. Correlation (Pearson's *r*) of activity patterns in each region for different task events. (*A*) FB and CH periods both separated by object and cycle. (*B*) FB period separated by object and cycle, CH period by location and cycle. Note that correlations on diagonal are 1.0 by definition (correlation of each activity vector with itself). cyc: cycle; o: object; and l: location.

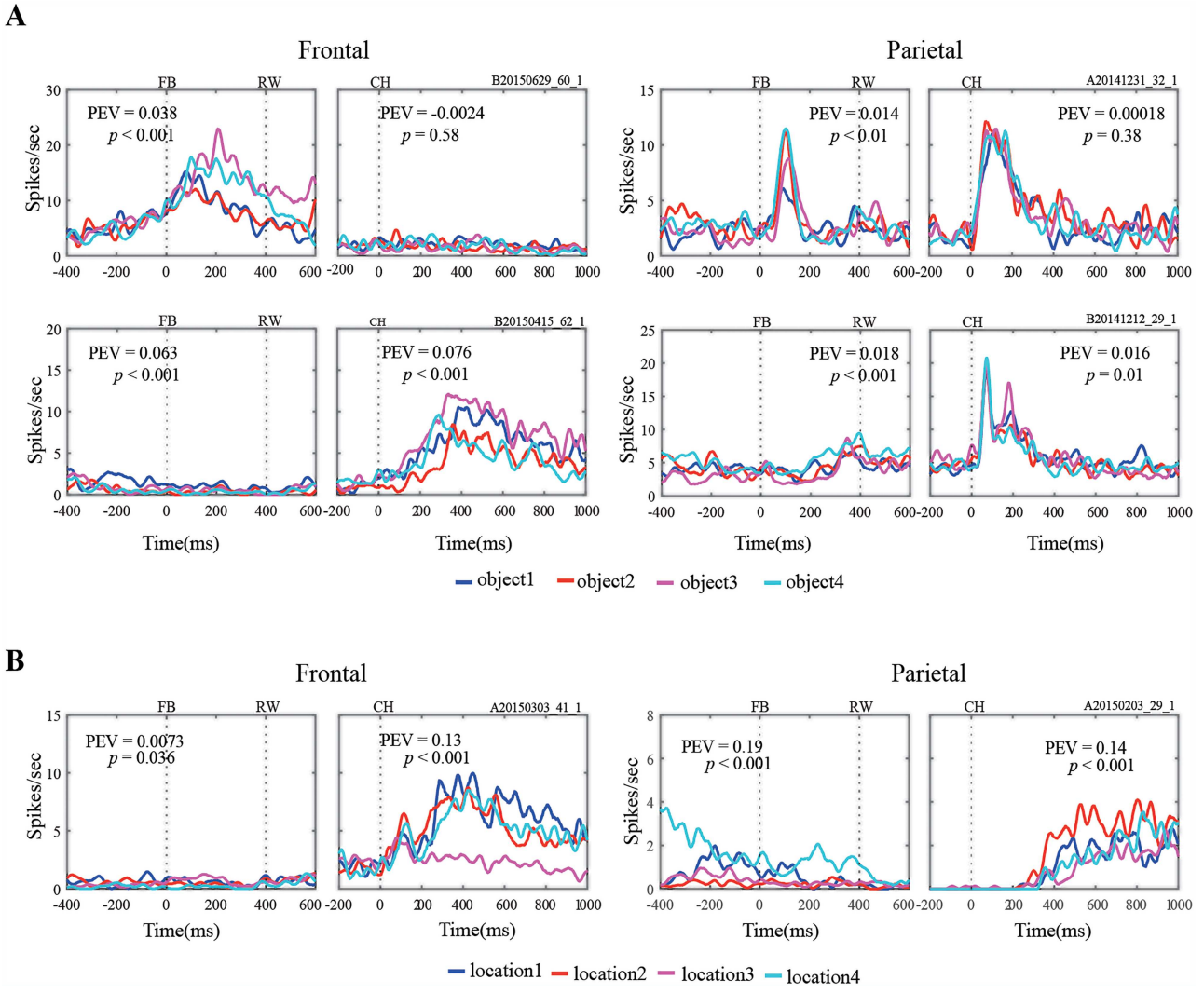

Figure 3. Activity of example neurons. (A) Object-selective cells. Left panel for each cell shows activity in feedback period (FB: onset of feedback; RW: average time of RW); right panel shows activity in choice period (CH: onset of choice display). In each panel, PEV and *p* value show main effect of object from ANOVA on windows −200 to +400 ms from FB, and +200 to +800 ms from CH. Upper left: dorsal frontal cell with object selectivity at FB; lower left: dorsal frontal cell with object selectivity at CH; upper right: inferior parietal cell with object selectivity at FB; and lower right: inferior parietal cell with mismatched object selectivity in the two periods. (B) Cells with location selectivity in the CH period. Left: ventral frontal; right: inferior parietal.

each recorded cell, with factors selected object × cycle × number of targets (1T, 2T). ANOVAs were performed on nonoverlapping 200 ms windows, covering the period −400 to +800 ms from FB. (Note that the reward itself was delivered between +350 and + 450 ms). For each recording region, target encoding was indexed by proportion of cells with a significant main effect of object ($p < 0.05$), as well as by mean PEV for the main effect (see Materials and Methods) across all recorded neurons. As each animal had two object sets, used in alternate problems in each session, analysis was performed separately for each set and the results averaged.

Results are shown in Figure 4A. Overall, around 10–15% of cells encoded object identity. Randomization tests (see Materials and Methods) on PEV values confirmed above-chance object encoding in all four regions (right panel, upper horizontal lines). Object coding was already established prior to receipt of the FB signal, and remained stable up to and following reward delivery. Object coding appeared somewhat stronger in frontal regions, and to compare frontal and parietal regions, we used Wilcoxon tests on the most selective 25% of cells (see Materials and Methods). For each comparison (dorsal, ventral frontal vs. inferior, superior parietal), the analysis showed periods of significantly stronger encoding in the frontal region (Fig. 4A, right panel, lower horizontal lines). Overall, object encoding was weakest in superior parietal neurons.

In 1T problems, the animal had to retain only a single target for the duration of each problem. In 2T problems, there was an increase in task complexity, with two targets to be retained and selected on successive trials. To examine the impact of task complexity, ANOVAs with factors object × cycle were separately carried out for 1T and 2T problems. Mean values of PEV from these two sets of ANOVAs are shown in Figure 4B. Overall, object selectivity at FB was stronger in 1T problems. For all regions except dorsal frontal, Wilcoxon tests (most selective 25% of cells; see Materials and Methods) showed periods of stronger object selectivity in the 1T case (Fig. 4B, horizontal lines).

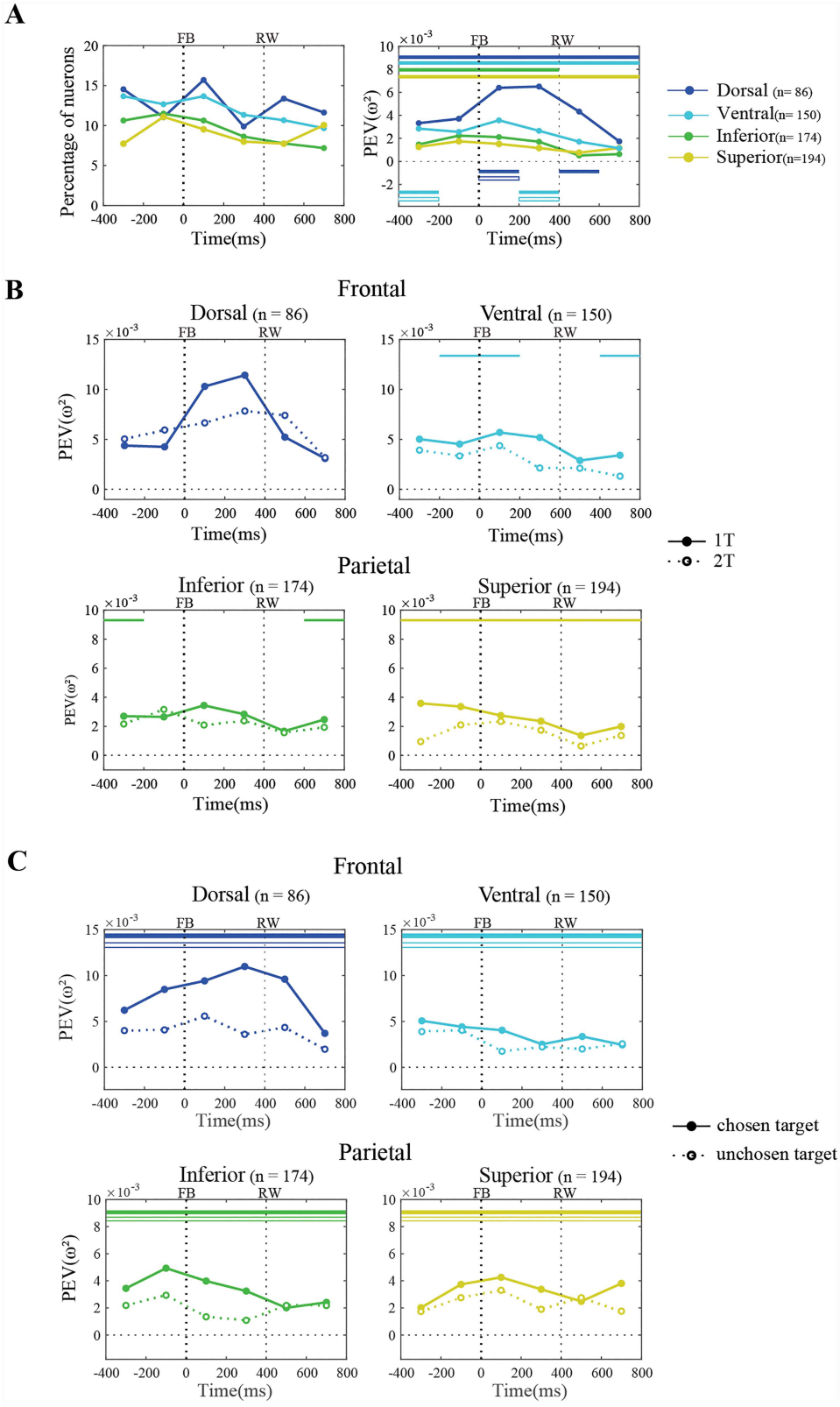

Figure 4. Object discrimination in the FB period. (A) All cycles: selectivity on target trials. Left: percentage of all analyzed cells with object selectivity. Right: mean PEV (ω^2) for object over all cells. Upper horizontal bars indicate periods of significant object selectivity (PEV > 0) in each region. Lower horizontal bars show significant differences between frontal and parietal regions. Blue: dorsal frontal vs. inferior (solid bars) and superior (open bars) parietal. Cyan: ventral frontal vs. inferior (solid bars) and superior (open bars) parietal. FB marks onset of FB signal. RW marks average time of RW. (B) All cycles: selectivity (mean PEV) for 1T (solid lines) and 2T (dotted lines) problems. Horizontal bars indicate significant difference between 1T and 2T. (C) Cycles 2–4, 2T task: selectivity for currently chosen target (solid lines) and other target in the current problem (dotted lines). Horizontal bars show significant selectivity for chosen (solid) and unchosen (open) target.

In a further analysis, we asked whether, in the 2T case, neural activity reflected not only the object selected on the current trial, but also the other target in the current problem. For this purpose, we focused on data from cycles 2–4, since on cycle 1, the other target might not yet be known. We used ANOVAs with factors current target × other target, pooling data over cycles to increase trial numbers. As the two object factors were not completely crossed, these ANOVAs derived only main effects, not interactions. Results are shown in Figure 4C. In all four recording areas, randomization tests on PEV (see Materials and Methods) showed significant information concerning not only the target chosen on the current trial, but also the other target held in memory.

In the FB phase, the requirement was to store the information received for control of future choices. At this trial phase, there was sustained, widespread encoding of object identity, beginning before FB and lasting until after the reward. Object encoding was stronger and more frequent in frontal than in parietal cortex. Matching behavioral results, the neurophysiological data also showed an effect of task complexity, with weaker object encoding when two different objects were to be learned and selected on different trials. Though FB concerned just the target chosen on the current trial, in this task phase, neural activity also carried information about a second target, held in memory for choice on other trials.

Selecting Targets in a Visual Display: Object Coding at Choice

Next, we turned to the choice period of each trial, when the monkey selected a target object from a four-alternative display. Here, we focused just on correct trials in cycles 2–4, when FB in cycle 1 had already indicated current target identities. In principle, object-selective activity could begin even before onset of the choice display, since the animal knew in advance the identity of the target object or objects. One possibility, for example, would be sustained or reawakened activity carried forward from the FB period of previous trials. Again, we used ANOVAs on 200 ms windows around onset of the choice display, with factors target object × target location × cycle. For each cell, the analysis was repeated twice, once for each object set, and the results averaged.

Results are shown in Figure 5. Corresponding results for location selectivity are shown for comparison. In frontal regions, there was some evidence for object selectivity, which began to appear only in the window 200–400 ms. As this was the same time window at which location information appeared, it suggests visual encoding of the target once it was found in the array, not an advance code used to direct attention. A similar, somewhat weaker result was seen in inferior parietal cortex. In superior parietal cortex, in contrast, there was no significant object information.

Our next question was whether, for individual cells, object preferences at FB and CH were congruent. To address this, we selected two analysis windows, −200 to +400 ms from FB, and + 200 to +800 ms from CH, selected to maximize object selectivity. For cells showing significant object selectivity in FB (ANOVA with factors object × number of targets, $p < 0.05$ for main effect of object), we examined responses during CH, and for cells showing significant object selectivity in CH, we examined responses during FB. Again, the analysis was carried out separately for the two object sets, and the results averaged.

Results are shown in Figure 6A. For each cell with object selectivity at FB, we defined a best and a worst object based on FB responses. We then calculated a mean firing rate during CH for these FB-defined best and worst objects, following normalization for each cell by dividing by the mean firing rate across objects × object sets × FB/CH periods. Mean CH responses for these FB-selective cells appear in the left panels of Figure 6A. For all four regions, responses to the FB-defined best and worst objects were indistinguishable in the CH period. Right panels in Figure 4A show results for the reverse analysis, defining object-selective cells, with their associated best and worst objects, from CH data, and measuring responses during FB. Again, responses to the CH-defined best and worst objects were indistinguishable in the FB period. These data show essentially independent object preferences in FB and CH phases, with a cell's object preference in one phase being unpredictable of preference in another. Results were closely similar if this analysis was repeated using a FB period of −400 to 0 ms, when the target object was still present on the screen, or using 0 to +400 ms, when the target had been replaced by the FB signal (see Supplementary Fig. 1). Thus, independence between FB and CH phases held irrespective of actual visual input in the FB period.

For comparison, Figure 6B assesses consistency of object preferences within a task phase. For each recorded cell, correct trials for each target object were divided into two sets, with alternate trials through the session assigned to each set (odd/even split). We then repeated an analysis similar to that in Figure 6A, but now selecting significant cells in one half of the data (e.g., FB period, odd trials), and measuring responses for the same task period in the other half (e.g., FB period, even trials). Results in Figure 6B are averaged across the two directions of analysis (select odd, measure even, and the reverse). For the FB period, in three of four recording areas, cells selected from one set of trials showed matched object preferences in the other set. The exception was superior parietal cortex, whose object preferences by this criterion were not stable. For the CH period, in agreement with the data in Figure 5, object preferences were very weak, with significant consistency only in the ventral frontal region.

Overall, these data tell against a model of visual object selection based on sustained or reawakened activity from the FB instruction period. Instead, encoding of target objects at FB, as the animal learned the rules of the current problem, was independent of encoding during visual processing, when attention was directed to the target object in a visual display.

Location Coding: Time-Course of Target Selection

In the next set of analyses, we focused on the process of locating the target in the CH display. Again, we wished to compare information coding and dynamics in frontal and parietal cortex, and to examine task complexity and attentional focus.

To track the time-course of location coding across recording areas, we performed ANOVAs on the data from each recorded cell, with factors target location × cycle × number of targets (1T, 2T). Compared with weak object coding, stronger location coding allowed us to examine the data at a finer time scale. ANOVAs were thus performed on nonoverlapping 50 ms windows, covering the period −200 to +1000 ms from display onset. For each region, target encoding was again indexed by proportion of cells with a significant main effect of location ($p < 0.05$), as well as by mean PEV across all recorded neurons.

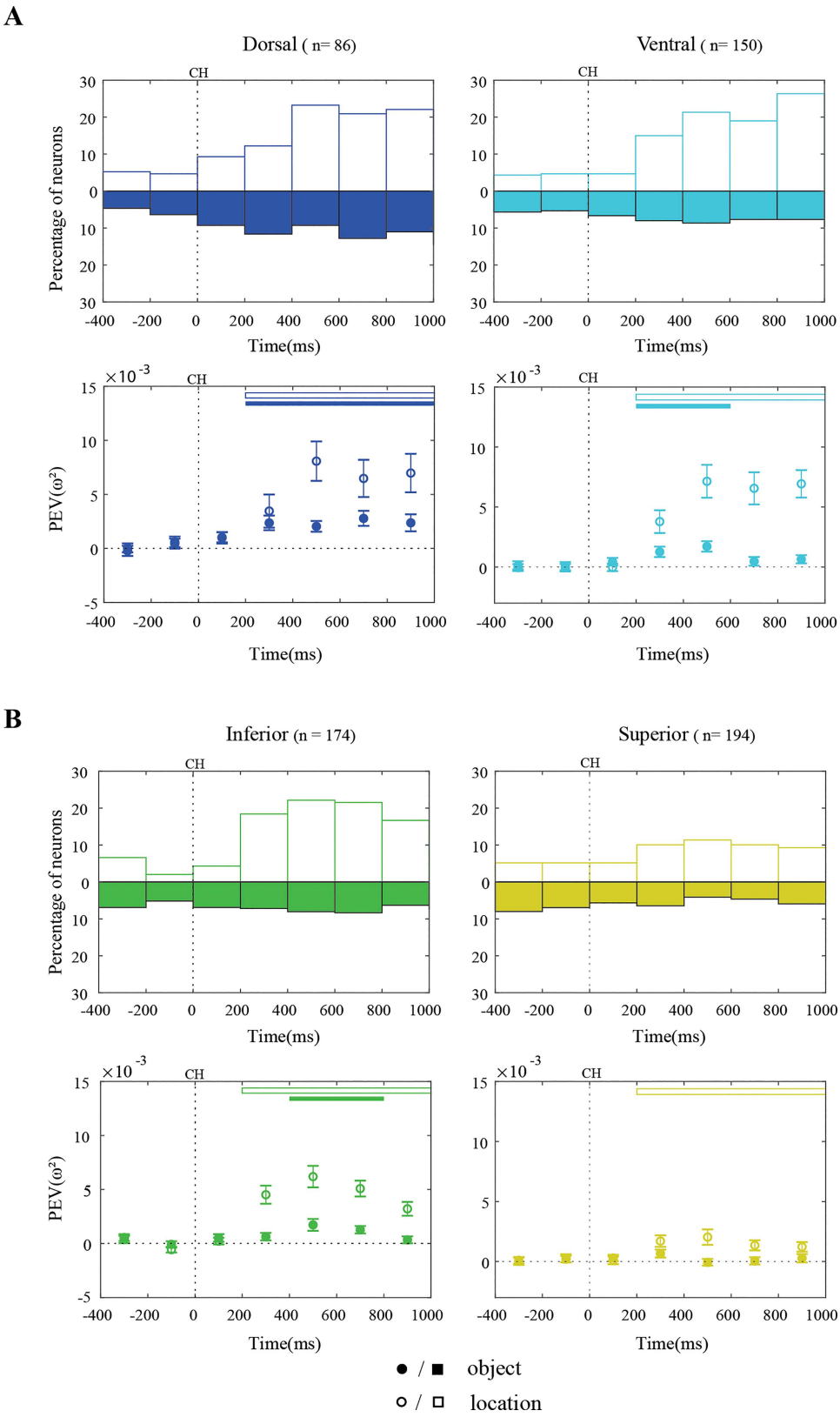

Figure 5. Object and location discrimination in the CH period. (A) Frontal cells. Upper: percentage of all analyzed cells with location (open bars) and object (filled bars) selectivity. Lower: mean PEV (ω^2) for location (open circles) and object (filled circles) over all cells. Upper horizontal bars indicate periods of significant location (open bars) and object (filled bars) selectivity. CH marks onset of choice array. (B) Parietal cells.

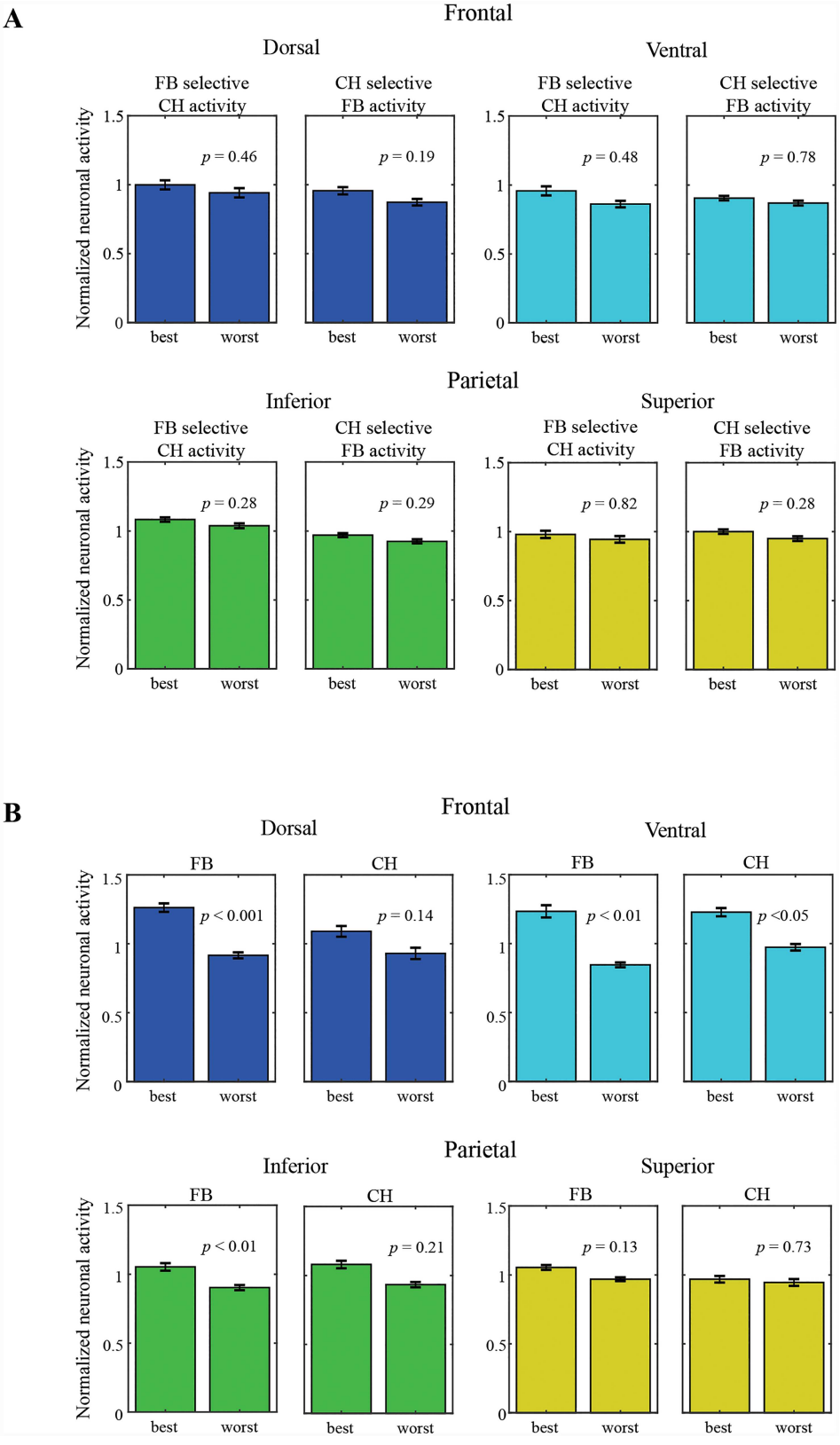

Figure 6. Differing object selectivity at FB and CH. (A) Mean activity in one period for cells identified as object-selective in the other. Left panel for each region: responses during CH for best and worst objects at FB. Right panel for each region: responses during FB for best and worst objects at CH. Data are mean normalized firing rates; *p* values show result of Wilcoxon tests comparing firing rates to best and worst objects. (B) Within each period, mean activity in one half of the data (odd or even trials) for cells identified as object-selective in the other half. Left panel for each region: FB period. Right panel for each region: CH period.

Results are shown in Figure 7A. In dorsal frontal, ventral frontal, and inferior parietal regions, encoding of target location became significant at or before the window 250–300 ms (right panel, upper horizontal lines). Across these three regions, there followed a parallel increase, both in percentage of significant cells and PEV, to a peak around 400 ms. Thereafter, location coding was sustained in both frontal lobe regions, but slowly declined in the inferior parietal cortex. Across the whole period, encoding of target location was weaker in the superior parietal cortex.

For statistical comparison between frontal and parietal regions, we again used Wilcoxon tests on the most selective 25% of cells (see Materials and Methods). Results are shown in the right panel of Figure 7A (lower horizontal lines). As expected, both frontal regions showed significant differences from superior parietal cortex throughout much of the time-course. For comparisons between frontal and inferior parietal regions, significant differences appeared toward the end of the analysis period, reflecting decay of location information in inferior parietal cortex.

Our next question concerned the stability of location preferences across the CH period. To address this, we used a temporal cross-generalization analysis (Stokes et al. 2013). Again, for each cell, correct trials for each target location were divided into odd and even sets. For every pair of locations, the cell's difference in firing rate was calculated twice, once for odd trials and once for even trials. For n cells, accordingly, we obtained two vectors of n firing rate differences, one for odd trials and the other for even trials. The correlation between these two vectors indicates the reliability of discrimination between this pair of locations across the whole neuron sample. The analysis was repeated in successive 50 ms bins from −200 to +1000 ms from display onset, indicating the development of location coding as the trial progressed. Furthermore, by correlating vectors across different time bins (e.g., odd trials at 100–150 ms, even trials for each time bin from −200 to +1000 ms), we can assess the temporal stability of location coding. This whole analysis was repeated for each pair of locations, and the results averaged across pairs.

The results are shown in Figure 7B. In the upper half of the figure, correlations are shown for matched time windows in odd and even trials. As expected, results closely match the PEV findings in Figure 7A, with reliable location coding beginning before 200 ms following display onset, increasing to a maximum over the following 200 ms, and thereafter remaining stable in prefrontal cortex but declining in parietal cortex. Again, across the time-course, the data show weakest coding in the superior parietal region.

The temporal cross-generalization results are shown in the lower part of each figure. Most importantly, for frontal and inferior parietal regions, the data suggest a stable spatial code beyond about 200 ms from display onset. Across the range 200−1000 ms, odd and even difference vectors were correlated, not only when they were drawn from the same time window, but also across the full range of time windows. As expected, correlations were uniformly weaker for the superior parietal region.

In part, sustained location coding over the choice period could reflect motor preparation. In many motor regions of monkey cortex (e.g., Gnadt and Andersen 1988; Johnson et al. 1996; Scott and Kalaska 1997; Scott et al. 1997; Snyder et al. 1997; Cui and Andersen 2007; Scherberger and Andersen 2007; Klaes et al. 2011), cells whose activity is linked to a particular movement show activity ramping up as the movement time approaches. To examine a possible role of motor preparation, we compared location coding in choice and movement periods. To this end, we repeated the temporal cross-generalization analysis, but now synchronized to the moment of KR. Results are shown in Figure 7C. In the period preceding KR, there was evidence of sustained, stable location coding (good cross-generalization between intervals preceding KR), especially in frontal cortex. These results are consistent with those already described for the choice period. In the period following KR, there was also strong location coding, especially in parietal cortex. Here, there was some evidence of temporal specificity, with stronger correlations on the diagonal (matched time window for odd and even data sets) than off-diagonal. Critically, however, there was no evidence for cross-generalization between periods before and after the KR. A cell's location preference before movement began was unrelated to its preference during the movement itself. These data give no suggestion that sustained location coding in the choice period reflected anticipatory movement-related activity.

Finally, we examined mean eye position in the period 0 to +1000 ms from onset of the CH display. For both animals, mean eye positions were closely similar for the four target locations (for horizontal position, greatest difference between any two target locations 0.10° and 0.23°, respectively, for the two animals; corresponding values for vertical position 0.11° and 0.22°) These small differences make it unlikely that discrimination of target locations in the neural data could be traced to differences in eye position.

Task Complexity: Attentional Focus in 2T Problems

In 2T problems, each display contained two potential targets. On the first trial of each cycle, the animal was free to choose either of these two. Once the first had been chosen, the animal was then required to choose the other. To examine the influence of competing targets in the display, we carried out two kinds of analysis.

First, we compared strength of location coding in 1T and 2T problems. For this purpose, we used ANOVAs on 50 ms windows as before, but now separately carried out on 1T and 2T data. Figure 8A shows mean PEVs across all recorded neurons. Overall, location coding was somewhat weaker in 2T problems, with significant differences in at least one time window for all four regions (Wilcoxon tests on most selective 25% of cells; see Materials and Methods).

Separating 2T trials into first or second within a cycle revealed no significant differences (data not shown).

Second, in 2T problems, we asked whether neural activity reflected, not only the location of the chosen target on the current trial, but also the location of the other target, also present in the display but not chosen on this trial. With the same analysis windows as before, we used ANOVAs with factors chosen target location × unchosen target location, pooling data over cycles to increase trial numbers. As the two location factors were not completely crossed, these ANOVAs derived only main effects, not interactions. Results are shown in Figure 8B. For all regions, the results show location coding entirely focused on the current

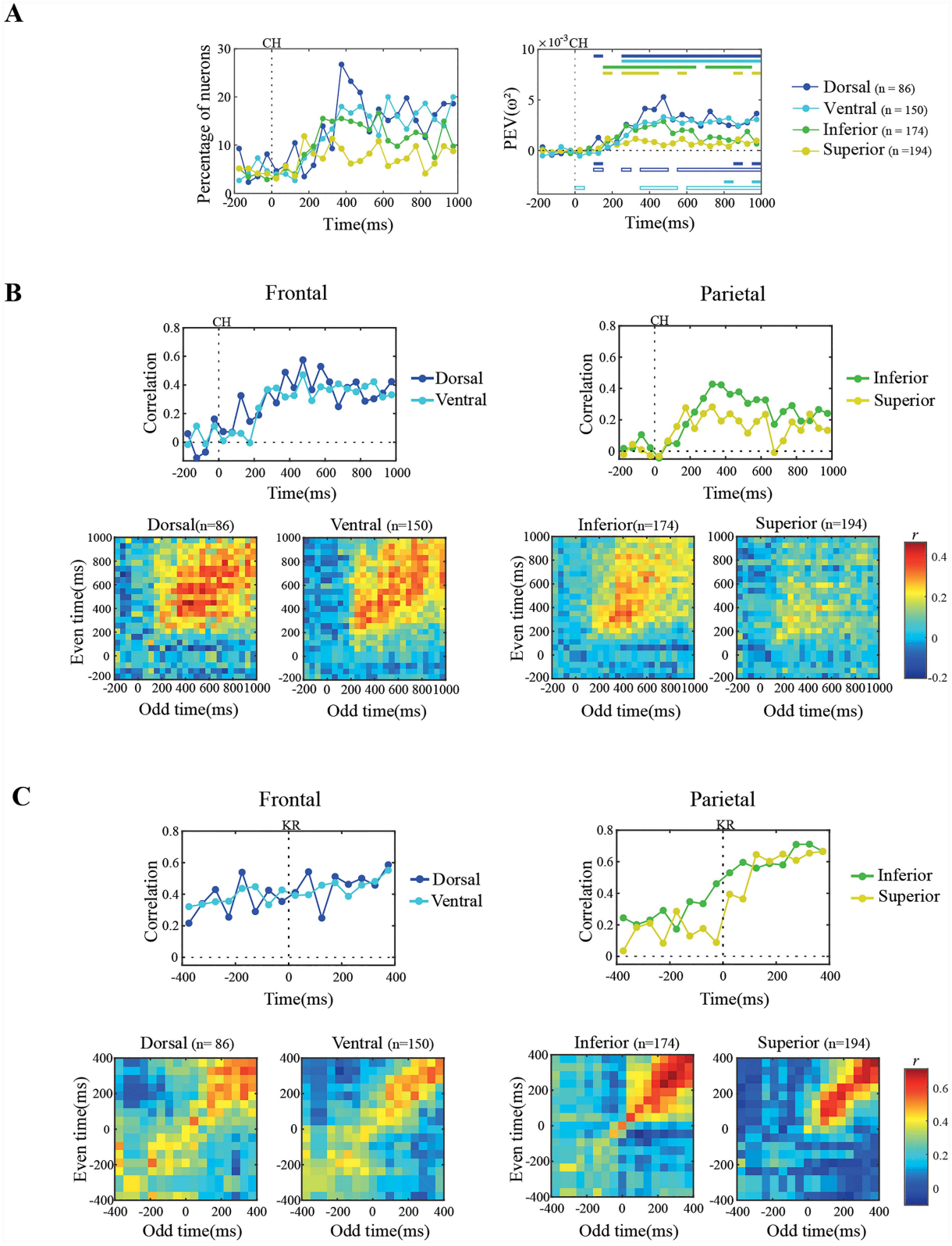

Figure 7. Location discrimination in the CH period. (A) Left: percentage of all analyzed cells with location selectivity. Right: mean PEV (ω^2) for location over all cells. Upper horizontal bars indicate periods of significant location selectivity in each region. Lower horizontal bars show significant differences between frontal and parietal regions. Blue: dorsal frontal vs. inferior (solid bars) and superior (open bars) parietal. Cyan: ventral frontal vs. inferior (solid bars) and superior (open bars) parietal. CH marks onset of choice array. (B) Top: reliability of location coding across data separated into two halves (odd and even trials) for each cell. For each pair of locations, location preference for each cell is separately calculated in odd and even trials. At each time-point, preferences in odd and even trials are correlated across all recorded cells. The figure shows results averaged across all six possible location pairs. CH marks onset of choice array. Bottom: stability of coding across time. Location preferences for odd and even trials are correlated for the same (diagonal; same data as top part of figure) or different (off-diagonal) time points. (C) Location coding synchronized on movement onset (KR).

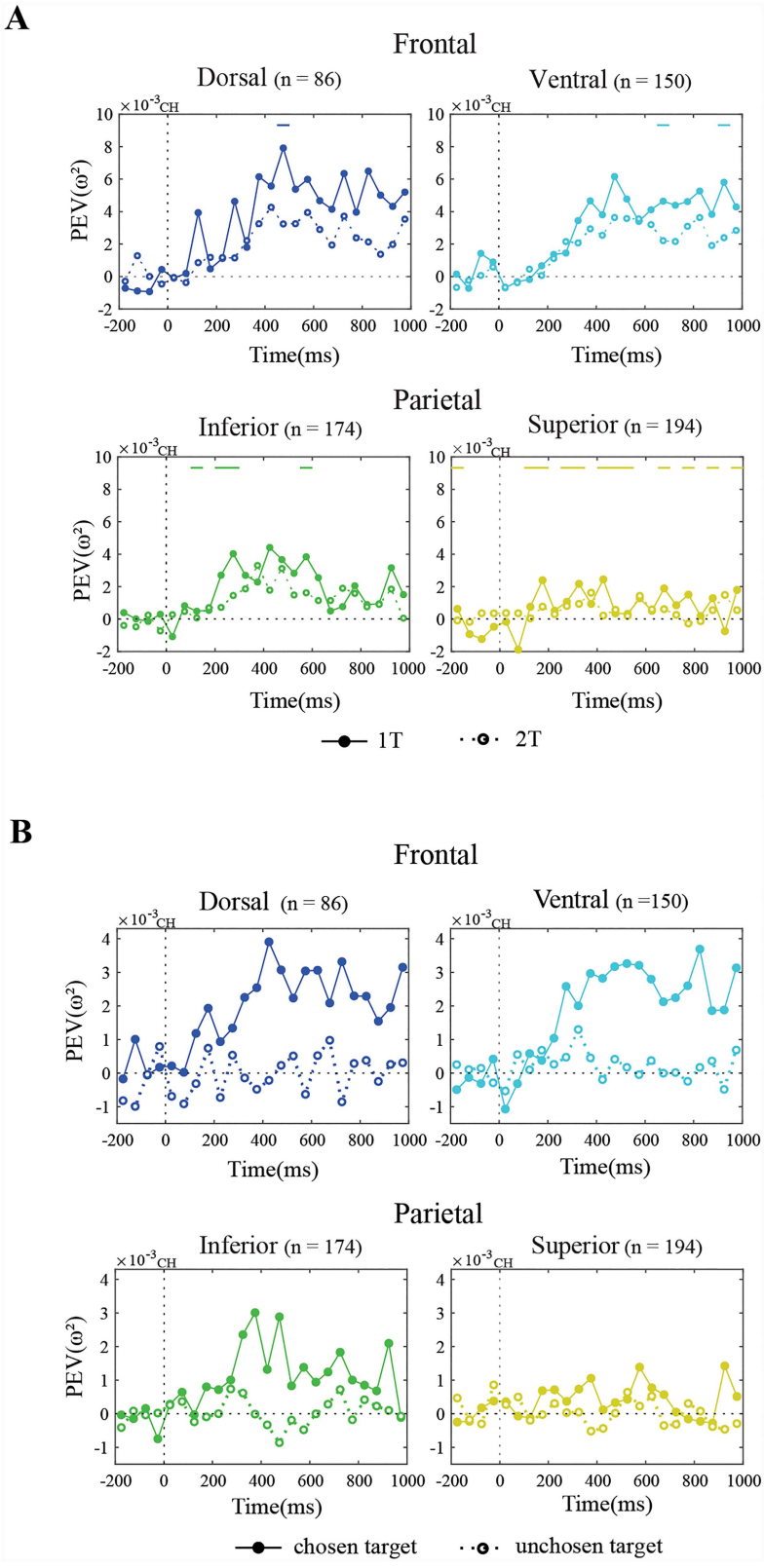

Figure 8. Attentional focus in the CH period. (A) Strength of location coding (mean PEV over all cells) for 1T(solid line) and 2T (dotted lines) trials. Top horizontal bars indicate significant differences between 1T and 2T. CH marks onset of choice array. (B) 2T problems: strength of coding (mean PEV over all cells) for chosen (solid lines) and unchosen (dotted lines) target locations on each trial.

(chosen) target, with PEV for the unchosen target remaining around zero throughout the display period.

Independence of Information Coding in Different Task Phases

Last, we asked whether overlapping or separate cell populations carry task-related activity at different task phases. For each cell, we measured PEV for object at FB (analysis window −200 to +400 ms from FB; cf. Fig. 2), and PEV for location at CH (analysis window +200 to +600 ms). Across cells, correlations between these values were close to zero or weakly positive in all regions (−0.02, −0.03, +0.25, and +0.01, respectively, for dorsal frontal, ventral frontal, inferior parietal, and superior parietal). A similar analysis concerned PEV for object at FB and CH, again showing low or weakly positive correlations (+0.38, +0.03, +0.19, and −0.02, respectively). Matching independent overall patterns of activity between task phases, these data suggest substantial independence in sets of cells carrying task-relevant trial information.

Discussion

In this study, we examined responses of frontal and parietal neurons in a complex object selection task. We compared neural activity across two phases of the task. After each selection, the FB signal acted as an instruction, indicating the rules of the current problem (whether the chosen object should be selected or avoided). At the CH phase, the requirement was to locate a current target in the visual display, and await a GO signal before reaching out to touch it. Our task has formal similarities to classic delayed match-to-sample, with one display indicating which object should be chosen in a subsequent set of alternatives. In our case, however, this delayed matching was embedded in a more complex overall task structure. With this design, we aimed to examine frontoparietal activity across successive task steps, calling for different cognitive processes, and by varying the number of targets, to ask how neural representation for a current choice is influenced by surrounding task complexity.

In line with the results of Sigala et al. (2008), our data showed independent patterns of neural activity at FB and CH phases. Furthermore, though object selectivity was found at both task phases, object preferences were rather unrelated across phases; a neuron's object preference at FB was not at all predictive of its response at CH, and vice versa. These results are quite unlike a classical, frontoparietal working memory signal, with sustained, object-selective activity linking initial presentation of a target to its later choice. Instead, they show "mixed selectivity," or activity driven by the conjunction of object and context (Mushiake et al. 2006; Sigala et al. 2008; Warden and Miller 2010; Hussar and Pasternak 2012; Rigotti et al. 2013; Naya et al. 2017). Many neurons too were selective for target location at the CH phase, but again, location coding was largely independent of object encoding during the rather different cognitive operations of FB. Thus, single neurons could be location-selective but not object-selective, object-selective but not location-selective, both or neither, in apparently random combinations.

It is widely supposed that neural activity in frontoparietal cortex acts as a cognitive control signal, assembling the set of processes required for a current mental operation (Norman and Shallice 1980; Miller and Cohen 2001). This control signal may influence activity across multiple brain systems, matching this activity to current task requirements. In this case, it makes sense that quite different control representations will be needed to direct different cognitive operations, in part implemented in different brain systems. At FB, the requirement was to store target identity for control of subsequent choices. At CH, the requirement was to select one from a number of objects in a visual display, directing visual attention to its location and preparing for the forthcoming reach. The data suggest independent patterns of frontoparietal activity implementing these different operations, and independent patterns of object selectivity binding each operation to its current target. In line with the classical computational problem of variable binding, cognitive control requires linking processing operations to their contents or arguments. In the present case, we suggest, different modulations of frontoparietal activity are needed to link object information to rule storage at FB and to visual selection at CH.

In our task, complexity had a substantial impact on the animal's behavior, with close to optimal performance in the 1T case, but errors persisting through repeated problem cycles in 2T. Corresponding effects of complexity in the neural data fit prior suggestions that, to some degree, frontoparietal cortex acts as a limited-capacity processor (Dehaene et al. 2003; Marois and Ivanoff 2005; Buschman et al. 2011). In the FB period, though the feedback received concerned only the target chosen on the current trial, information concerning this target was diminished when a second target was held in memory for selection on other trials. At this point, furthermore, information on the identity of this second target emerged in neural activity. At CH, similarly, the location of the current target was less accurately represented in 2T problems, though in this case, there was no suggestion of encoding the location of the second target, present in the display but not currently selected. These results show that, as frontoparietal activity reorganizes to encode events of the current trial, its accuracy is limited by the total complexity of information to be used across the whole series of trials. In several respects, our results resemble data reported by Watanabe and Funahashi (2014) in a spatial delayed-saccade task. In that study, the target stimulus for the delayed saccade was presented while the animal focused attention on a second, concurrent task, with the saccade only made after the concurrent task was complete. Both behavioral and neurophysiological data showed evidence of limited processing capacity, with reduced accuracy, and reduced frontal signaling of the target location, as the complexity of the concurrent task increased. At the same time, there was evidence of focus on the current cognitive operation, with frontal encoding of the delayed-saccade target decaying during concurrent task performance, then re-emerging as the animal returned to the saccade task.

Resembling sustained delay activity in traditional working memory tasks, previous studies of visual search have shown sustained activity, indicating the target for the current trial, in brain regions including inferior temporal (Chelazzi et al. 1993) and lateral frontal (Bichot et al. 2015) cortex. Logically, target selection in search must be controlled by some advance information concerning the target to be sought (Duncan and Humphreys 1989; Bundesen 1990). In our case, however, there was no evidence for this kind of sustained target code in advance of the CH display. As noted above, object selectivity at FB, when the target was originally defined, was unrelated to object selectivity while processing the search display. Furthermore, object coding at CH began only after display onset, with a time-course closely following the time-course of target location encoding. Such findings suggest, not an advance signal guiding attention to the chosen target, but a signal driven by visual information

from the selected display item itself. One possibility is that sustained, target-selective activity could have been present in other brain regions, directing target selection. Another possibility is the kind of "silent" code envisaged in several recent accounts of top–down control and working memory (Postle 2015). Such a silent code, for example, could be implemented by short-term changes in synaptic weights rather than sustained firing patterns (Mongillo et al. 2008; for a recent proposal on how silent and active information coding could be combined, see Lundqvist et al. 2016). As others have suggested (Lewis-Peacock et al. 2012; Stokes 2015), sustained firing may be a principal mechanism of working memory storage when only a single stimulus is to be remembered for immediate use. In more complex settings, such as the task used here, silent mechanisms may predominate (Lundqvist et al. 2018).

Our results show largely overlapping properties in dorsal frontal, ventral frontal, and inferior parietal neurons. In all three regions, activity patterns were approximately independent at FB and CH phases. All three showed object selectivity at both FB and CH, though at FB, object information was somewhat stronger in frontal regions. At CH, all three regions showed representation of target location arising in the period 200–400 ms from display onset, then sustained in a stable, nonmotor form up to the time of the response. Like object coding at FB, the stability of location coding at CH was somewhat stronger in frontal cortex, in line with prior data (Fuster and Alexander 1971; Miller et al. 1996) and models (Wang 2001) suggesting strong information maintenance in frontal neurons. Largely, parallel development of location representations in frontal and parietal cortex is consistent with previous studies of visual search, measuring latencies for location discrimination in individual frontal and parietal neurons. Though these studies sometimes show differences in mean latency between regions (Buschman and Miller 2007; Katsuki and Constantinidis 2012; Meyers et al. 2018), there is little consistency in the direction of such differences, and in all cases, substantial overlap in frontal and parietal latency distributions.

Beyond visual search, many previous neurophysiological and imaging studies show similar activity and neural properties in lateral frontal and inferior parietal cortex (e.g., Chafee and Goldman-Rakic 1998; Cabeza and Nyberg 2000; Duncan 2010; Goodwin et al. 2012; Salazar et al. 2012; Suzuki and Gottlieb 2013). Many authors suggest that cognitive control is implemented by distributed patterns of activity across lateral frontal and inferior parietal cortex, perhaps as part of a wider "multiple-demand" system including dorsomedial frontal and insular cortex (Duncan 2010), and reflecting dense connectivity between these regions (e.g., Petrides and Pandya 1984). In contrast to widespread involvement in many cognitive activities, superior parietal cortex has a more focused role in visuomotor control, including reaching to visual targets (Colby and Duhamel 1991; Kalaska 1996; Colby and Goldberg 1999; Eskandar and Assad 1999). Consistent with this, in superior parietal cortex, we found strong encoding of target location at the time of the monkey's reach, but only weak encoding during the prior selection interval, weak object signals at FB, and a complete absence of object signals at CH. Working memory is an important aspect of cognitive control, allowing an animal to escape from control by immediate sensory input (Goldman-Rakic 1988; Fuster 1989). More broadly, however, cognitive control requires assembly of the component steps of complex behavior, with each step integrating relevant goals, stimuli, processing operations, outputs etc. For each task step, our data show a distinctive frontoparietal activity pattern, independent of the pattern for other steps, and with its own, step-specific encoding rules for task-relevant information. The step-specific activity pattern, we suggest, serves to marshal the appropriate cognitive operations, while modulations of that pattern direct these operations to appropriate cognitive content. In this way, frontoparietal activity patterns assemble the successive episodes of complex mental activity.

Supplementary Material

Supplementary material is available at *Cerebral Cortex* online.

Notes

This work was supported by the Medical Research Council (UK, programme SUAG/002/RG91365), the Wellcome Trust (grant 101092/Z/13/Z) to JD, and a JSPS Postdoctoral Fellowship for Research Abroad to KW.

We thank the Oxford biomedical service staff and veterinarians for their expert animal husbandry, advice on surgery, and postoperative care. *Conflict of Interest*: None declared.

References

Bichot NP, Heard MT, DeGennaro EM, Desimone R. 2015. A source for feature-based attention in the prefrontal cortex. *Neuron*. 88:832–844.

Brincat SL, Siegel M, von Nicolai C, Miller EK. 2018. Gradual progression from sensory to task-related processing in cerebral cortex. *Proc Natl Acad Sci U S A*. 115:E7202–E7211.

Bundesen C. 1990. A theory of visual attention. *Psychol Rev*. 97:523–547.

Buschman TJ, Denovellis EL, Diogo C, Bullock D, Miller EK. 2012. Synchronous oscillatory neural ensembles for rules in the prefrontal cortex. *Neuron*. 76:838–846.

Buschman TJ, Miller EK. 2007. Top-down versus bottom-up control of attention in the prefrontal and posterior parietal cortices. *Science*. 315:1860–1862.

Buschman TJ, Siegel M, Roy JE, Miller EK. 2011. Neural substrates of cognitive capacity limitations. *Proc Natl Acad Sci U S A*. 108:11252–11255.

Cabeza R, Nyberg L. 2000. Imaging cognition II: an empirical review of 275 PET and fMRI studies. *J Cogn Neurosci*. 12:1–47.

Cavada C, Goldman-Rakic PS. 1989. Posterior parietal cortex in rhesus monkey: II. Evidence for segregated corticocortical networks linking sensory and limbic areas with the frontal lobe. *J Comp Neurol*. 287:422–445.

Cavanagh SE, Towers JP, Wallis JD, Hunt LT, Kennerley SW. 2018. Reconciling persistent and dynamic hypotheses of working memory coding in prefrontal cortex. *Nat Commun*. 9:3498.

Chafee MV, Goldman-Rakic PS. 1998. Matching patterns of activity in primate prefrontal area 8a and parietal area 7ip neurons during a spatial working memory task. *J Neurophysiol*. 79:2919–2940.

Chelazzi L, Miller EK, Duncan J, Desimone R. 1993. A neural basis for visual search in inferior temporal cortex. *Nature*. 363:345–347.

Chiang FK, Wallis JD. 2018. Spatiotemporal encoding of search strategies by prefrontal neurons. *Proc Natl Acad Sci U S A*. 115:5010–5015.

Colby CL, Duhamel JR. 1991. Heterogeneity of extrastriate visual areas and multiple parietal areas in the macaque monkey. *Neuropsychologia*. 29:517–537.

Colby CL, Goldberg ME. 1999. Space and attention in parietal cortex. *Annu Rev Neurosci*. 22:319–349.

Constantinidis C, Funahashi S, Lee D, Murray JD, Qi XL, Wang M, Arnsten AFT. 2018. Persistent spiking activity underlies working memory. *J Neurosci*. 38:7020–7028.

Crowe DA, Goodwin SJ, Blackman RK, Sakellaridi S, Sponheim SR, MacDonald AW 3rd, Chafee MV. 2013. Prefrontal neurons transmit signals to parietal neurons that reflect executive control of cognition. *Nat Neurosci*. 16:1484–1491.

Cui H, Andersen RA. 2007. Posterior parietal cortex encodes autonomously selected motor plans. *Neuron*. 56:552–559.

Dehaene S, Sergent C, Changeux JP. 2003. A neuronal network model linking subjective reports and objective physiological data during conscious perception. *Proc Natl Acad Sci U S A*. 100:8520–8525.

Duncan J. 2010. The multiple-demand (MD) system of the primate brain: mental programs for intelligent behavior. *Trends Cogn Sci*. 14:172–179.

Duncan J. 2013. The structure of cognition: attentional episodes in mind and brain. *Neuron*. 80:35–50.

Duncan J, Humphreys GW. 1989. Visual search and stimulus similarity. *Psychol Rev*. 96:433–458.

Duncan J, Parr A, Woolgar A, Thompson R, Bright P, Cox S, Bishop S, Nimmo-Smith I. 2008. Goal neglect and Spearman's g: competing parts of a complex task. *J Exp Psychol Gen*. 137:131–148.

Eskandar EN, Assad JA. 1999. Dissociation of visual, motor and predictive signals in parietal cortex during visual guidance. *Nat Neurosci*. 2:88–93.

Freedman DJ, Assad JA. 2006. Experience-dependent representation of visual categories in parietal cortex. *Nature*. 443:85–88.

Freedman DJ, Riesenhuber M, Poggio T, Miller EK. 2001. Categorical representation of visual stimuli in the primate prefrontal cortex. *Science*. 291:312–316.

Funahashi S, Bruce CJ, Goldman-Rakic PS. 1989. Mnemonic coding of visual space in the monkey's dorsolateral prefrontal cortex. *J Neurophysiol*. 61:331–349.

Fuster JM. 1989. *The prefrontal cortex-anatomy, physiology, and neuropsychology of the frontal lobe*. New York: Raven Press.

Fuster JM, Alexander GE. 1971. Neuron activity related to short-term memory. *Science*. 173:652–654.

Fuster JM, Bauer RH, Jervey JP. 1982. Cellular discharge in the dorsolateral prefrontal cortex of the monkey in cognitive tasks. *Exp Neurol*. 77:679–694.

Genovesio A, Brasted PJ, Wise SP. 2006. Representation of future and previous spatial goals by separate neural populations in prefrontal cortex. *J Neurosci*. 26:7305–7316.

Gnadt JW, Andersen RA. 1988. Memory related motor planning activity in posterior parietal cortex of macaque. *Exp Brain Res*. 70:216–220.

Goldman-Rakic PS. 1988. Topography of cognition: parallel distributed networks in primate association cortex. *Annu Rev Neurosci*. 11:137–156.

Goodwin SJ, Blackman RK, Sakellaridi S, Chafee MV. 2012. Executive control over cognition: stronger and earlier rule-based modulation of spatial category signals in prefrontal cortex relative to parietal cortex. *J Neurosci*. 32:3499–3515.

Hussar CR, Pasternak T. 2012. Memory-guided sensory comparisons in the prefrontal cortex: contribution of putative pyramidal cells and interneurons. *J Neurosci*. 32:2747–2761.

Johnson PB, Ferraina S, Bianchi L, Caminiti R. 1996. Cortical networks for visual reaching: physiological and anatomical organization of frontal and parietal lobe arm regions. *Cereb Cortex*. 6:102–119.

Kalaska JF. 1996. Parietal cortex area 5 and visuomotor behavior. *Can J Physiol Pharmacol*. 74:483–498.

Katsuki F, Constantinidis C. 2012. Early involvement of prefrontal cortex in visual bottom-up attention. *Nat Neurosci*. 15:1160–1166.

Klaes C, Westendorff S, Chakrabarti S, Gail A. 2011. Choosing goals, not rules: deciding among rule-based action plans. *Neuron*. 70:536–548.

Lapish CC, Durstewitz D, Chandler LJ, Seamans JK. 2008. Successful choice behavior is associated with distinct and coherent network states in anterior cingulate cortex. *Proc Natl Acad Sci U S A*. 105:11963–11968.

Lewis-Peacock JA, Drysdale AT, Oberauer K, Postle BR. 2012. Neural evidence for a distinction between short-term memory and the focus of attention. *J Cogn Neurosci*. 24:61–79.

Luck SJ, Vogel EK. 1997. The capacity of visual working memory for features and conjunctions. *Nature*. 390:279–281.

Lundqvist M, Herman P, Miller EK. 2018. Working memory: delay activity, yes! Persistent activity? Maybe Not. *J Neurosci*. 38:7013–7019.

Lundqvist M, Rose J, Herman P, Brincat SL, Buschman TJ, Miller EK. 2016. Gamma and Beta bursts underlie working memory. *Neuron*. 90:152–164.

Mante V, Sussillo D, Shenoy KV, Newsome WT. 2013. Context-dependent computation by recurrent dynamics in prefrontal cortex. *Nature*. 503:78–84.

Marois R, Ivanoff J. 2005. Capacity limits of information processing in the brain. *Trends Cogn Sci*. 9:296–305.

Meyers EM, Liang A, Katsuki F, Constantinidis C. 2018. Differential processing of isolated object and multi-item pop-out displays in LIP and PFC. *Cereb Cortex*. 28:3816–3828.

Miller EK. 2000. The prefrontal cortex and cognitive control. *Nat Rev Neurosci*. 1:59–65.

Miller EK, Cohen JD. 2001. An integrative theory of prefrontal cortex function. *Annu Rev Neurosci*. 24:167–202.

Miller EK, Erickson CA, Desimone R. 1996. Neural mechanisms of visual working memory in prefrontal cortex of the macaque. *J Neurosci*. 16:5154–5167.

Mongillo G, Barak O, Tsodyks M. 2008. Synaptic theory of working memory. *Science*. 319:1543–1546.

Mushiake H, Saito N, Sakamoto K, Itoyama Y, Tanji J. 2006. Activity in the lateral prefrontal cortex reflects multiple steps of future events in action plans. *Neuron*. 50: 631–641.

Naya Y, Chen H, Yang C, Suzuki WA. 2017. Contributions of primate prefrontal cortex and medial temporal lobe to temporal-order memory. *Proc Natl Acad Sci U S A*. 114:13555–13560.

Norman D, Shallice T. 1980. *Attention to action: willed and automatic control of behavior (report no.8006)*. San Diego: University of California, Center for Human Information Processing.

Oemisch M, Westendorff S, Everling S, Womelsdorf T. 2015. Interareal spike-train correlations of anterior cingulate and dorsal prefrontal cortex during attention shifts. *J Neurosci*. 35:13076–13089.

Parthasarathy A, Herikstad R, Bong JH, Medina FS, Libedinsky C, Yen SC. 2017. Mixed selectivity morphs population codes in prefrontal cortex. *Nat Neurosci*. 20:1770–1779.

Petrides M, Pandya DN. 1984. Projections to the frontal cortex from the posterior parietal region in the rhesus monkey. *J Comp Neurol*. 228:105–116.

Postle BR. 2015. The cognitive neuroscience of visual short-term memory. *Curr Opin Behav Sci*. 1:40–46.

Raposo D, Kaufman MT, Churchland AK. 2014. A category-free neural population supports evolving demands during decision-making. *Nat Neurosci*. 17:1784–1792.

Rigotti M, Barak O, Warden MR, Wang XJ, Daw ND, Miller EK, Fusi S. 2013. The importance of mixed selectivity in complex cognitive tasks. *Nature*. 497:585–590.

Rigotti M, Ben Dayan Rubin D, Wang XJ, Fusi S. 2010. Internal representation of task rules by recurrent dynamics: the importance of the diversity of neural responses. *Front Comput Neurosci*. 4:24.

Rishel CA, Huang G, Freedman DJ. 2013. Independent category and spatial encoding in parietal cortex. *Neuron*. 77:969–979.

Salazar RF, Dotson NM, Bressler SL, Gray CM. 2012. Content-specific fronto-parietal synchronization during visual working memory. *Science*. 338:1097–1100.

Scherberger H, Andersen RA. 2007. Target selection signals for arm reaching in the posterior parietal cortex. *J Neurosci*. 27:2001–2012.

Scott SH, Kalaska JF. 1997. Reaching movements with similar hand paths but different arm orientations. I. Activity of individual cells in motor cortex. *J Neurophysiol*. 77:826–852.

Scott SH, Sergio LE, Kalaska JF. 1997. Reaching movements with similar hand paths but different arm orientations. II. Activity of individual cells in dorsal premotor cortex and parietal area 5. *J Neurophysiol*. 78:2413–2426.

Sigala N, Kusunoki M, Nimmo-Smith I, Gaffan D, Duncan J. 2008. Hierarchical coding for sequential task events in the monkey prefrontal cortex. *Proc Natl Acad Sci U S A*. 105: 11969–11974.

Smolensky P. 1990. Tensor product variable binding and the representation of symbolic structures in connectionist systems. *Artificial Intelligence*. 46:159–216.

Snyder LH, Batista AP, Andersen RA. 1997. Coding of intention in the posterior parietal cortex. *Nature*. 386:167–170.

Stokes MG. 2015. 'Activity-silent' working memory in prefrontal cortex: a dynamic coding framework. *Trends Cogn Sci*. 19:394–405.

Stokes MG, Kusunoki M, Sigala N, Nili H, Gaffan D, Duncan J. 2013. Dynamic coding for cognitive control in prefrontal cortex. *Neuron*. 78:364–375.

Suzuki M, Gottlieb J. 2013. Distinct neural mechanisms of distractor suppression in the frontal and parietal lobe. *Nat Neurosci*. 16:98–104.

Wang XJ. 2001. Synaptic reverberation underlying mnemonic persistent activity. *Trends Neurosci*. 24:455–463.

Warden MR, Miller EK. 2010. Task-dependent changes in short-term memory in the prefrontal cortex. *J Neurosci*. 30:15801–15810.

Wasmuht DF, Spaak E, Buschman TJ, Miller EK, Stokes MG. 2018. Intrinsic neuronal dynamics predict distinct functional roles during working memory. *Nat Commun*. 9: 3499.

Watanabe K, Funahashi S. 2014. Neural mechanisms of dual-task interference and cognitive capacity limitation in the prefrontal cortex. *Nat Neurosci*. 17:601–611.